Front. Phys. 13(1), 138205 (2018)
https://doi.org/10.1007/s11467-017-0699-1

RESEARCH ARTICLE

Dynamics of supercooled confined water measured by deep inelastic neutron scattering

Vincenzo De Michele[1], Giovanni Romanelli[2], Antonio Cupane[1,†]

[1] *Dipartimento di Fisica e Chimica, Università di Palermo, Viale delle Scienze Ed. 18, 90128 Palermo, Italy*
[2] *ISIS Facility, Rutherford Appleton Laboratory, Chilton, Didcot, Oxfordshire OX11 0QX, UK*
Corresponding author. E-mail: [†] *antonio.cupane@unipa.it*
Received March 6, 2017; accepted May 8, 2017

In this paper, we present the results of deep inelastic neutron scattering (DINS) measurements on supercooled water confined within the pores (average pore diameter $\sim$ 20 Å) of a disordered hydrophilic silica matrix obtained through hydrolysis and polycondensation of the alkoxide precursor Tetra-Methyl-Ortho-Silicate via the sol-gel method. Experiments were performed at two temperatures (250 K and 210 K, i.e., before and after the putative liquid–liquid transition of supercooled confined water) on a "wet" sample with hydration $h \sim 40\%$ w/w, which is high enough to have water-filled pores but low enough to avoid water crystallization. A virtually "dry" sample at $h \sim 7\%$ was also investigated to measure the contribution of the silica matrix to the neutron scattering signal. As is well known, DINS measurements allow the determination of the mean kinetic energy and the momentum distribution of the hydrogen atoms in the system and therefore, allow researchers to probe the local structure of supercooled confined water. The main result obtained is that at 210 K the hydrogen mean kinetic energy is equal or even slightly higher than at 250 K. This is at odds with the predictions of a semi-empirical harmonic model recently proposed to describe the temperature dependence of the kinetic energy of hydrogen in water. This is a new and very interesting result, which suggests that at 210 K, the water hydrogens experience a stiffer intermolecular potential than at 250 K. This is in agreement with the liquid–liquid transition hypothesis.

Keywords confined water, liquid–liquid transition, hydrogen mean kinetic energy, silica xerogel

PACS numbers 61.43.Gt, 64.70.Ja, 61.05.fg, 82.30.Rs, 82.33.Ln

1 Introduction

The dynamics and structure of liquid water continuously attracts attention and raises the interests of researchers. Water is not a simple liquid; many of its physical properties exhibit anomalous behavior, which is particularly evident at low temperatures such as in the supercooled state. The increase in isothermal compressibility and isobaric specific heat with decreasing temperature, as well as the increase in the self-diffusion coefficient with increasing pressure, are among the most striking anomalies of supercooled water [1, 2]. Various hypotheses have been proposed to explain the origin of the above anomalies; perhaps the most interesting (and challenging) one is the existence of a second critical point of water at low temperatures, which was originally predicted by molecular dynamics simulations of ST2 water [3]. A key experimental observation confirming the liquid–liquid critical point (LLCP) hypothesis is the detection of a so-called fragile-to-strong crossover (FSC) at 225 K and ambient pressure in the dynamical properties of supercooled confined water [4–6]. In fact, the crossover is detected at a temperature separating a predominantly low density state of liquid (LDL) water at lower temperatures (with a local structure characterized by large volume, low entropy, and stiffer intermolecular potential due to a fully developed network of tetrahedral hydrogen bonds), from a predominantly high density state of liquid (HDL) water at higher temperatures (with a local structure characterized by smaller volume, larger entropy, and softer intermolecular potential due to a distorted, bent, and possibly interpenetrated net-

*Special Topic: Water and Water Systems (Eds. F. Mallamace, R. Car, and Limei Xu).

work of hydrogen bonds). Although recent experiments and simulations on bulk water [7, 8], nano-confined water [5, 9], and on protein hydration water [6, 10–12] support the above hypothesis, an intense debate regarding this is still ongoing in literature [13, 14] and the validity of the hypothesis may be considered an open question. Here, we report the results of a DINS experiment performed at 250 K and 210 K on supercooled water confined within the pores of a disordered hydrophilic silica matrix (silica xerogel). The aim of the experiment is to exploit the unique possibility offered by the DINS technique of obtaining information on the mean kinetic energy and momentum distribution [15] of the hydrogen atoms of the system and thereby, to probe the dynamics and the intermolecular potential experienced by the supercooled confined water molecules. The main result obtained is that, notwithstanding a 40 K temperature decrease, at 210 K (where water should be predominantly in the LDL state), the hydrogen mean kinetic energy is equal or even slightly higher than at 250 K (where water should be predominantly in the HDL state). This suggests that confined water molecules experience a stiffer intramolecular potential at 210 K than at 250 K, which is in agreement with the liquid–liquid transition hypothesis [16]. Because confinement within nanometer-sized porous hydrophilic matrices closely mimics the confinement conditions experienced by water molecules in crowded biological systems, we believe that the present results enhance the understanding of the physical properties of water, and they may be of relevance to other applied scientific fields such as biophysics, biopreservation, and pharmaceutics.

2 Materials and methods

2.1 Samples

Hydrated silica xerogels were obtained by hydrolysis and polycondensation of an aqueous suspension of the alkoxide precursor Tetra-Methyl-Ortho-Silicate (TMOS) according to the sol-gel procedure already described in previous publications of our group [17, 18]. The following protocol was used: an aqueous suspension containing 75% v/v TMOS (Sigma Aldrich), 22.5% v/v H_2O, and 2.5% v/v HCl $0,2N$ was sonicated for 20 min in an ice bath; immediately after sonication, it was mixed with H_2O in a 1 : 1 proportion (by volume). After careful mixing, the final suspension was poured into suitable plastic containers and stored at room temperature to complete the hydrolysis and polycondensation processes. Polycondensation is a much slower process compared to hydrolysis under the conditions used in our study (acid catalysis). The above protocol was adopted to minimize the number of silanol (SiOH) groups present on the pore surfaces. Solid transparent samples were obtained with this procedure and were left to age for at least two months. The sample hydration level h (defined as $h = [gr\mathrm{H_2O}]/[gr\mathrm{SiO_2}]$) decreases slowly with time due to excess water evaporation and can be easily determined by weight measurements. When the desired hydration was reached (in our case $h \sim 40\%$), the sample was crunched to obtain a fine powder and accurately sealed to avoid further water loss. Hydrated xerogel powders thus obtained consisted of a disordered, porous, three-dimensional SiO_2 matrix characterized by a broad pore size distribution with average value of approximately 20 Å [17]. The pore walls probably had a small amount of silanol groups left behind by incomplete condensation. Water is confined within the pores of the matrix. Two samples with hydration levels of $h \sim 40\%$ and $h \sim 7\%$ were investigated in this study. This last sample was obtained after prolonged vacuum dehydration at $\sim 60°C$ and was used to determine the contribution of the "dry" silica matrix to the neutron scattering signal.

2.2 DINS measurements

DINS measurements were performed with the VESUVIO instrument at the ISIS spallation neutron source (Rutherford Appleton Laboratory, UK) with energy transfer $\hbar\omega$ within the range of 1 eV to 65 eV and wavevector transfer Q within the range of 30 $Å^{-1}$ to 200 $Å^{-1}$ [15]. The samples were first placed in thin aluminum sachets to prevent the powder from falling to the bottom of the cell, which can result in loss of signal. The sachets were then contained in 60 mm × 60 mm ×1 mm aluminum indium-sealed cells. A standard close cycle refrigerator was used to control the cell temperature to within ±0.1 K.

2.3 Data analysis

As is well known, the VESUVIO spectrometer collects neutrons scattered at the various Q values using the time of flight (*tof*) technique [15]. Raw data were corrected for contributions arising from the gamma-ray background [19] and from multiple scattering [20] using standard procedures available at VESUVIO [21]. Moreover, the contributions of aluminum, silicon, and oxygen atoms (that appear as an unresolved peak, which is well separated from the hydrogen peak) were also subtracted by a standard routine to obtain the corrected hydrogen *tof* spectra. In the next step of the data analysis, the West scaling variable [22] $y = \frac{M}{\hbar Q}\left(\omega - \frac{\hbar Q^2}{2M}\right)$ was introduced and *tof* spectra were converted in y space to obtain the experimental response function $F(y, Q)$, which is also called the hydrogen neutron Compton profile (NCP) [15, 23].

The experimental NCP for the lth individual detector, $F_l(y,Q)$, was expressed as the convolution of the proton response function $J_l(y,Q)$ and the resolution function of the lth detector $R_l(y,Q)$. For $J_l(y,Q)$, we used a Gram–Charlier expansion [15] truncated to the first non-zero Hermite coefficient c_4 plus a correction term proportional to the Hermite polynomial H_3 with coefficient c_1 to take into account the final state effects (FSE) [24]. A global fit over the entire set of fixed angle spectra (performed in the range -30 Å$^{-1} \leq y \leq 30$ Å^{-1} using a bin width of 0.5 Å^{-1}) enables to obtain the best values of the parameters σ, c_4, and c_1. Finally, from the σ values of the global fit, we obtained the mean kinetic energy of the hydrogen atoms in our samples as $\langle EK \rangle = \frac{3\hbar^2\sigma^2}{2M}$ [15]. The proton radial momentum distribution is obtained from the NCP averaged over all the detectors following the method described in Ref. [25]. For the wet sample ($h = 0.40$), data taken at the two temperatures (210 K and 250 K) were analyzed separately; for the dry sample ($h = 0.07$), due to the much lower signal, data at 210 K and at 250 K were summed and analyzed using a Gaussian NCP with FSE correction.

3 Results and discussion

Figure 1 shows the NCP averaged over all the detectors obtained for the various samples investigated here. Note that the rather weak signal obtained for the "dry" sample did not allow separate analysis of the data at 250 K and 210 K. These were further averaged before the analysis to increase the signal to noise ratio. Therefore, data in the lower panel of Fig. 1 refer to the dry sample at the average temperature of approximately 230 K.

The continuous lines in Fig. 1 are the NCP calculated using the parameter values obtained from the global fit, as reported in the Materials and Methods section; the fitting quality is quite good, as shown by the residuals (green lines in Fig. 1). It is possible to calculate the momentum distributions $n(p)$ and the radial momentum distributions $4\pi p^2 n(p)$ from the parameter values reported in Table 1 [15]; the values for the latter are reported in Fig. 2 for the two samples.

It is interesting to compare our results with the previous results obtained from similar systems [25, 26]. In particular, we have no clear evidence of a bimodal proton radial momentum distribution. This may be either due to the different temperatures used in the experiments, or more likely due to the very different procedures of sample preparation that, in our case, was carefully tuned to minimize the presence of silanol groups on the pore surface of the matrix. Regarding the values of parameters σ and $\langle EK \rangle$, no direct comparisons with previous results are possible in view of the rather different tem-

Table 1 Parameter values obtained from the global fits, as reported in the Materials and Methods section.

Sample	c_1	c_4	σ (Å^{-1})	E_K (meV)
Wet; $T=210$ K	0.010 ± 0.001	0.15 ± 0.02	5.01 ± 0.04	157 ± 3
Wet; $T=250$ K	0.012 ± 0.001	0.13 ± 0.02	4.98 ± 0.03	156 ± 2
Dry	0.007 ± 0.002		4.33 ± 0.03	118 ± 2

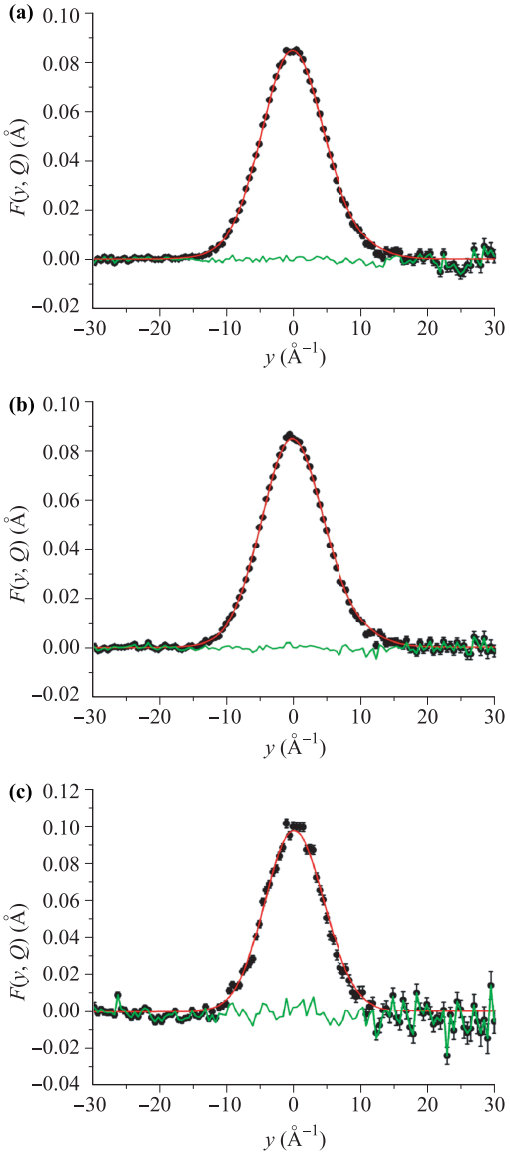

Fig. 1 Hydrogen NCP for the wet sample at 210 K **(a)**, at 250 K **(b)**, and for the dry sample **(c)**. Black points with error bars: Experimental response function, $F(y)$, averaged over all the detectors. Red continuous lines: Theoretical averaged response functions calculated using the best values of parameters σ, c_4, and c_1 obtained from the global fittings. Green continuous lines: Residuals.

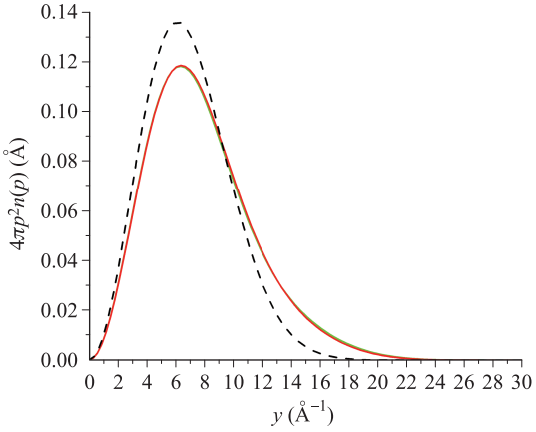

Fig. 2 Spherical average of the momentum distribution of hydrogen atoms in the investigated samples. Continuous lines: Wet sample at 250 K (*red*) and 210 K (*green*); Dashed black line: Dry sample.

peratures used in the experiments. The most interesting and intriguing result obtained in the present study concerns the temperature dependencies of parameters σ and $\langle EK \rangle$. In fact, data in Table 1 show that for the wet sample, no substantial difference in the mean kinetic energy of the hydrogen atoms of confined water is observed at the two temperatures, notwithstanding a 40 K temperature variation. To better understand the significance of this result, it is worth comparing it with the predictions of a semi-empirical model recently proposed in literature [27, 28] to describe the temperature dependence of the kinetic energy of hydrogen in water. The model uses harmonic approximation and assumes decoupling between translation, rotation-libration, and internal vibrations of the water molecules. Because the water in our samples is confined, we neglected the contributions of free translation and rotation and considered only the contributions arising from low frequency collective vibrations and librations and from the stretching and bending normal modes of the H_2O molecule. We used the following expression based on the approach of Ref. [27]:

$$EK = 3\int_0^{\nu_{\max}} g(\nu)\left[\frac{h\nu}{2}\left(\frac{1}{e^{\frac{h\nu}{k_B T}}-1}+\frac{1}{2}\right)\right]d\nu + \sum_{j=1}^{3} S_j \frac{h\nu_j}{2}\left(\frac{1}{e^{\frac{h\nu_j}{k_B T}}-1}+\frac{1}{2}\right). \quad (1)$$

The contributions of low frequency vibrations/librations are contained in the normalized distribution $g(\nu)$; S_j are the fractions of the kinetic energy share of the H-atom in each of the three normal modes and their values were taken from Ref. [27]; the sum in Eq. (1) is calculated over the three normal modes of the water molecule. We used the vibrational frequencies of 3280 cm^{-1}, 3490 cm^{-1}, and 1645 cm^{-1} for symmetric stretching, asymmetric stretching, and bending, respectively. These values are in substantial agreement with the frequency values reported by Mallamace and coworkers [29, 30] for water confined in MCM-41 silica matrix and for the hydration water of lysozyme. For the distribution $g(\nu)$, we used the vibrational density of states of the same system measured at 257 K by Cupane *et al.* [31]. A comparison between our data and the model data is reported in Fig. 3. Considering the assumptions and approximations made in the calculations, the very good agreement at 250 K may be considered as somewhat fortuitous. Figure 3 clearly shows that a decrease in mean kinetic energy of water hydrogen with decreasing temperature is expected, which is contrary to what is actually observed; in fact, the experiment shows that at 210 K the mean kinetic energy is equal or even slightly higher than at 250 K.

This suggests that at 210 K the water hydrogens experience a stiffer intermolecular potential than at 250 K, in agreement with the putative LDL → HDL crossover occurring at approximately 225 K in supercooled confined water. Note that the LDL → HDL crossover has been shown to influence the collective vibrational dynamics of confined water, as evidenced by the temperature [31, 32] and pressure [33] dependence of the boson peak (BP) measured with inelastic neutron scattering. The decrease in the hydrogen mean kinetic energy between 210 K and 250 K reported in this paper is in overall agreement with the "disappearance" of the BP (more specifically: the inflection point in the temperature dependence of the BP intensity) at 225 K in confined water.

Although the results of this study are new and stimulating, they still need to be considered as preliminary.

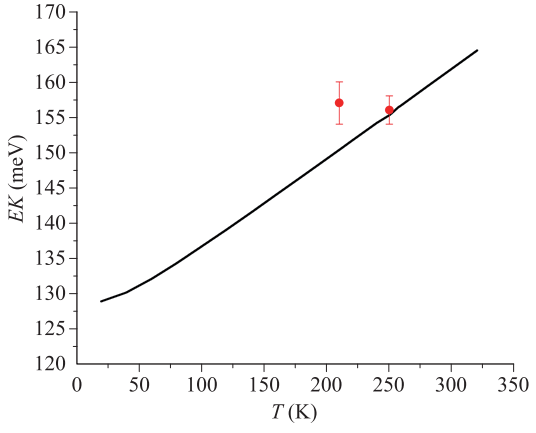

Fig. 3 Points (red points): Hydrogen mean kinetic energy as derived from the experimentally determined σ values. Continuous line: Temperature dependence of the hydrogen mean kinetic energy in water as predicted by the semi-empirical harmonic model described in the text.

Further experiments are needed to draw more definitive conclusions; in particular, the full temperature dependence of the hydrogen mean kinetic energy in the range of 180 − 290 K should be measured. Such experiments are currently being planned [34].

Acknowledgements V. D. M. and A. C. thank the members of the Molecular Biophysics and Nanotechnology group at the University of Palermo, Italy, for useful discussions and their indirect financial support. Financial support from Italian CNR (Dipartimento di Scienze Fisiche e Tecnologie della Materia) is also gratefully acknowledged; in fact, this work was supported under the CNR-STFC Agreement (2014–2020) concerning collaboration in scientific research at the ISIS pulsed neutron and muon source.

References

1. P. G. Debenedetti, Supercooled and glassy water, *J. Phys.: Condens. Matter* 15(45), R1669 (2003)
2. A. Nilsson and L. G. M. Pettersson, The structural origin of anomalous properties of liquid water, *Nat. Commun.* 6, 8998 (2015)
3. P. H. Poole, F. Sciortino, U. Essmann, and H. E. Stanley, Phase behaviour of metastable water, *Nature* 360(6402), 324 (1992)
4. L. Liu, S. H. Chen, A. Faraone, C. W. Yen, and C. Y. Mou, Pressure dependence of fragile-to-strong transition and a possible second critical point in supercooled confined water, *Phys. Rev. Lett.* 95(11), 117802 (2005)
5. S. H. Chen, F. Mallamace, C. Y. Mou, M. Broccio, C. Corsaro, A. Faraone, and L. Liu, The violation of the Stokes–Einstein relation in supercooled water, *Proc. Natl. Acad. Sci. USA* 103(35), 12974 (2006)
6. G. Schirò, M. Fomina, and A. Cupane, Communication: Protein dynamical transition vs. liquid–liquid phase transition in protein hydration water, *J. Chem. Phys.* 139(12), 121102 (2013)
7. J. C. Palmer, F. Martelli, Y. Liu, R. Car, A. Z. Panagiotopoulos, and P. G. Debenedetti, Metastable liquid–liquid transition in a molecular model of water, *Nature* 510(7505), 385 (2014)
8. J. A. Sellberg, C. Huang, T. A. McQueen, N. D. Loh, H. Laksmono, D. Schlesinger, R. G. Sierra, D. Nordlund, C. Y. Hampton, D. Starodub, D. P. DePonte, M. Beye, C. Chen, A. V. Martin, A. Barty, K. T. Wikfeldt, T. M. Weiss, C. Caronna, J. Feldkamp, L. B. Skinner, M. M. Seibert, M. Messerschmidt, G. J. Williams, S. Boutet, L. G. M. Pettersson, M. J. Bogan, and A. Nilsson, Ultrafast X-ray probing of water structure below the homogeneous ice nucleation temperature, *Nature* 510(7505), 381 (2014)
9. Z. Wang, K. Ito, J. B. Leão, L. Harriger, Y. Liu, and S. H. Chen, Liquid–liquid phase transition and its phase diagram in deeply-cooled heavy water confined in a nanoporous silica matrix, *J. Phys. Chem. Lett.* 6(11), 2009 (2015)
10. S. H. Chen, L. Liu, E. Fratini, P. Baglioni, A. Faraone, and E. Mamontov, Observation of fragile-to-strong dynamic crossover in protein hydration water, *Proc. Natl. Acad. Sci. USA* 103(24), 9012 (2006)
11. M. Fomina, G. Schirò, and A. Cupane, Hydration dependence of myoglobin dynamics studied with elastic neutron scattering, differential scanning calorimetry and broadband dielectric spectroscopy, *Biophys. Chem.* 185, 25 (2014)
12. G. Schirò and A. Cupane, Anharmonic activations in proteins and peptide model systems and their connection with supercooled water thermodynamics, *Il Nuovo Cimento C* 39(3), 305 (2016)
13. D. T. Limmer and D. Chandler, The putative liquid–liquid transition is a liquid–solid transition in atomistic models of water, *J. Chem. Phys.* 135(13), 134503 (2011)
14. A. K. Soper, Density profile of water confined in cylindrical pores in MCM-41 silica, *J. Phys.: Condens. Matter* 24(6), 064107 (2012)
15. C. Andreani, D. Colognesi, J. Mayers, G. F. Reiter, and R. Senesi, Measurement of momentum distribution of light atoms and molecules in condensed matter systems using inelastic neutron scattering, *Adv. Phys.* 54(5), 377 (2005)
16. H. E. Stanley, P. Kumar, L. Xu, Z. Yan, M. G. Mazza, S. V. Buldyrev, S. H. Chen, and F. Mallamace, The puzzling unsolved mysteries of liquid water: Some recent progress, *Physica A* 386(2), 729 (2007)
17. M. Cammarata, M. Levantino, A. Cupane, A. Longo, A. Martorana, and F. Bruni, Structure and dynamics of water confined in silica hydrogels: X-ray scattering and dielectric spectroscopy studies, *Eur. Phys. J. E* 12(Suppl. 1), S63 (2003)
18. M. D'Amico, G. Schirò, A. Cupane, L. D'Alfonso, M. Leone, V. Militello, and V. Vetri, High fluorescence of thioflavin T confined in mesoporous silica xerogels, *Langmuir* 29(32), 10238 (2013)
19. J. Mayers, Calculation of background effects on the VESUVIO eV neutron spectrometer, *Meas. Sci. Technol.* 22(1), 015903 (2011)
20. J. Mayers, A. L. Fielding, and R. Senesi, Multiple scattering in deep inelastic neutron scattering: Monte Carlo simulations and experiments at the ISIS eVS inverse geometry spectrometer, *Nucl. Instrum. Methods Phys. Res. A* 481(1–3), 454 (2002)
21. J. Mayers, User Guide to VESUVIO Data Analysis: Programs for Powders and Liquids, ISIS Facility, 2010
22. G. B. West, Electron scattering from atoms, nuclei and nucleons, *Phys. Rep.* 18(5), 263 (1975)
23. G. I. Watson, Neutron Compton scattering, *J. Phys.: Condens. Matter* 8(33), 5955 (1996)

24. M. Krzystyniak, A. G. Seel, S. E. Richards, M. J. Gutmann, and F. Fernandez-Alonso, Mass-selective neutron spectroscopy beyond the proton, *J. Phys. Conf. Ser.* 571, 012002 (2014)
25. C. Pantalei, R. Senesi, C. Andreani, P. Sozzani, A. Comotti, S. Bracco, M. Beretta, P. E. Sokol, and G. Reiter, Interaction of single water molecules with silanols in mesoporous silica, *Phys. Chem. Chem. Phys.* 13(13), 6022 (2011)
26. V. Garbuio, C. Andreani, S. Imberti, A. Pietropaolo, G. F. Reiter, R. Senesi, and M. A. Ricci, Proton quantum coherence observed in water confined in silica nanopores, *J. Chem. Phys.* 127(15), 154501 (2007)
27. Y. Finkelstein and R. Moreh, Temperature dependence of the proton kinetic energy in water between 5 and 673 K, *Chem. Phys.* 431–432, 58 (2014)
28. G. Romanelli, F. Fernandez-Alonso, and C. Andreani, The harmonic picture of nuclear mean kinetic energies in heavy water, *J. Phys. Conf. Ser.* 571, 012003 (2014)
29. F. Mallamace, M. Broccio, C. Corsaro, A. Faraone, D. Majolino, V. Venuti, L. Liu, C. Y. Mou, and S. H. Chen, Evidence of the existence of the low-density liquid phase in supercooled, confined water, *Proc. Natl. Acad. Sci. USA* 104(2), 424 (2007)
30. F. Mallamace, S.H. Chen, M. Broccio, C. Corsaro, V. Crupi, D. Majolino, V. Venuti, P. Baglioni, E. Fratini, C. Vannucci, and H. E. Stanley, Role of the solvent in the dynamical transitions of proteins: The case of the lysozyme-water system., *J. Chem. Phys.* 127(4), 045104 (2007)
31. A. Cupane, M. Fomina, and G. Schirò, The boson peak of deeply cooled confined water reveals the existence of a low-temperature liquid–liquid crossover, *J. Chem. Phys.* 141, 18C510 (2014)
32. Z. Wang, K. H. Liu, P. Le, M. Li, W. S. Chiang, J. B. Leão, J. R. D. Copley, M. Tyagi, A. Podlesnyak, A. I. Kolesnikov, C. Y. Mou, and S. H. Chen, Boson peak in deeply cooled confined water: A possible way to explore the existence of the liquid-to-liquid transition in water, *Phys. Rev. Lett.* 112(23), 237802 (2014)
33. Z. Wang, A. I. Kolesnikov, K. Ito, A. Podlesnyak, and S. H. Chen, Pressure effect on the boson peak in deeply cooled confined water: Evidence of a liquid–liquid transition, *Phys. Rev. Lett.* 115(23), 235701 (2015)
34. A. Cupane, V. De Michele, and G. Romanelli, *ISIS experiment* 1710456, 2017